Chapter 4

Insights into the Structure-Activity Relationship of Alkynyl-Coumarinyl Ethers as Selective MAO-B Inhibitors Using Molecular Docking

Yassir Boulaamane[1,*]
Mohammed Reda Britel[1]
and Amal Maurady[1,2]
[1]Laboratory of Innovative Technologies, National School of Applied Sciences of Tangier, Abdelmalek Essaddi University, Tetouan, Morocco
[2]Faculty of Sciences and Techniques of Tangier, Abdelmalek Essaddi University, Tetouan, Morocco

Abstract

Coumarins are considered a highly privileged and versatile scaffold by medicinal chemists. A considerable number of studies have highlighted the synthesis and the various pharmacological activities of coumarins as promising drug candidates for treating neurodegenerative diseases such as Parkinson's and Alzheimer's disease. A wide range of compounds based on the coumarin ring system have been found to possess biological activities such as anticonvulsant, antiviral, anti-inflammatory, antibacterial, antioxidant as well as monoamine oxidase inhibitory properties. Their promise as a novel drug for neurodegenerative diseases is demonstrated by many drug candidates that made it to clinical trials such as nodakenin that have been potent for demoting memory impairment. This study focuses on some synthesized alkynyl-coumarinyl

* Corresponding Author's Email: boulaamane.yassir@etu.uae.ac.ma

In: The Chemistry of Coumarin
Editor: Scott R. Sheley
ISBN: 979-8-88697-560-4
© 2023 Nova Science Publishers, Inc.

ethers with promising MAO-B inhibitory activity and selectivity and aims to elucidates the molecular interactions of ether-connected coumarins behind obtaining remarkably high MAO-B selectivity using molecular docking. Structure-activity relationship analysis revealed a common interaction between the selective coumarin inhibitors consisting of hydrogen bonding with Tyr-188 and Cys-172. Our findings might open new opportunities to explore for developing novel highly selective MAO-B inhibitors for the treatment of neurodegenerative diseases.

Keywords: coumarin, neurodegenerative diseases, molecular docking, monoamine oxidase, structure-activity relationship

Introduction

Parkinson's disease (PD) is considered the second most frequent neurodegenerative disorder after Alzheimer's disease [1]. PD is defined by the progressive loss of dopaminergic neurons in the substantia nigra pars compacta (SNpc) of the mid brain [2]. Current treatments for PD are levodopa, which remains the gold standard, dopamine agonists and catechol-O-methyl transferase (COMT)/monoamine oxidase (MAO) inhibitors [3]. Monoamine Oxidase (MAO) (EC 1.4.3.4) is a mitochondrial flavoprotein attached to neurons outer-membrane that catalyses the oxidative deamination of neurotransmitters and biogenic amines [4]. MAO exists in two forms; MAO-A and MAO-B that share about 70% of their sequence identity, but differ in their tissue distribution, substrate, and inhibitor preferences [5]. MAO-A inhibitors are used as antidepressants, while selective MAO-B inhibitors have proven to be efficient in treating AD and PD symptoms. Moreover, they may act as neuroprotective agents by limiting the release of free radical species and hence decrease the progression of the disease [6,7].

MAO-A preferentially metabolizes serotonin while MAO-B preferentially deaminates 2-phenylethylamine and benzylamine. Dopamine, norepinephrine, and epinephrine are metabolized by both isoforms [8].

During aging, the expression of MAO-B increases in the brain and relates to an enhanced dopamine metabolism that produce reactive oxygen species (ROS) such as hydrogen peroxide (H_2O_2) resulting in oxidative damage and apoptotic signalling events [9].

MAO-A (PDB ID: 2Z5Y) is expressed as a monomer while MAO-B is formed of two monomers, both formed of a globular domain attached to the outer neuronal membrane through a C-terminal helix [10, 11]. The active site

is located in the substrate fixing domain and is formed by the residues: Tyr-60, Pro-102, Pro-104, Leu-164, Phe-168, Leu-171, Cys-172, Ile-198, Ile-199, Gln-206, Ile-316, Tyr-326, Phe-343, Tyr-398 and Tyr-435 (10). Specific residues in MAO-B that are not present in MAO-A are: Leu-171, Cys-172, Ile-199 and Tyr-326 [11].

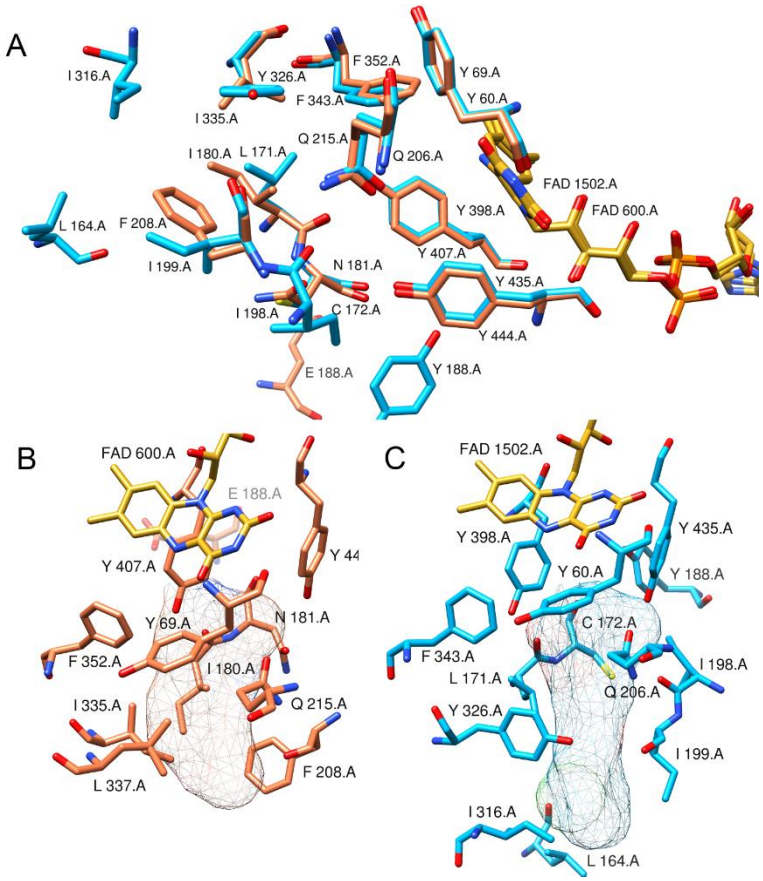

Figure 1. (A) Superimposition of the binding sites of hMAO-A (PDB ID: 2Z5Y) (coral) and hMAO-B (PDB ID: 2V61) (deep sky blue). (B, C) Binding surfaces of MAO-A (B) and MAO-B (C) are shown in mesh representation.

Coumarins are considered a privileged scaffold in medicinal chemistry due to its peculiar physicochemical properties and the synthetic accessibility to transform it into a wide plethora of functionalized coumarins [12]. Coumarins have been broadly studied for developing new MAO inhibitors

displaying a wide range of selectivity for MAO-B [13]. A recent study has reported that alkynyl coumarinyl ethers are able to inhibit MAO enzymes at nanomolar concentrations ranging from 0.58 nM to 1790 nM with a MAO-B selectivity reaching a value of over 3400-fold [14].

To develop new potent and highly selective MAO-B inhibitors, molecular modelling was used to get an insight on the possible molecular mechanisms of previously synthetised and biologically evaludated alkynyl-coumarinyl ethers [14].

Molecular docking study was carried out to investigate the structural conformations of the selected compounds with human MAO-B. Structure-activity relationship (SAR) analysis was conducted to identify the key molecular interactions that may enhance the selectivity for MAO-B.

Materials and Methods

Protein Preparation

The crystallographic structure of the human MAO-B (in complex with the selective inhibitor 7-(3-chlorobenzyloxy)-4-(methylamino) methyl-coumarin, C18) was obtained from the RCSB Protein Data Bank (http://www.rcsb.org/pdb/) (PDB ID: 2V61, resolution = 1.7 Å) and was prepared for molecular docking [11]. Co-crystallized ligand and water molecules were removed as they weren't involved in ligand binding. Chain B was removed and only chain A was kept along with the FAD cofactor as it plays an important role in catalysing the oxidative deamination of monoamines [15].

Chemical Structures Preparation

The selected coumarin derivatives were converted to chemical structures from their IUPAC nomenclature using MarvinSketch 20.9, 2020 (http://www.chemaxon.com) program. Explicit hydrogens and 3D coordinates were also generated. The Amber's antechamber module included with UCSF Chimera was used for energy minimisation of selected ligands, 100 steps of steepest descent minimization was performed, followed by 10 steps of conjugate gradient minimisation based on the AMBER ff14SB force field [16]. The chemical structures of coumarins are reported in Table 1 and 2.

Table 1. Chemical structures of R^1 derivatives and their MAO inhibitory activities [14]

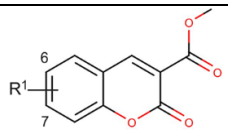

Compound	Nomenclature	R^1	Structure	SI
1a	Methyl 2-oxo-7-(prop-2-ynyloxy)-2H-chromene-3-carboxylate	$CH_2C{\equiv}CH$	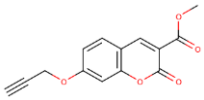	0.88
2a	Methyl 2-oxo-7-(but-3-ynyloxy)-2H-chromene-3-carboxylate	$(CH_2)_2C{\equiv}CH$	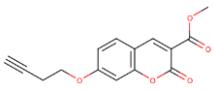	3.17
3a	Methyl 2-oxo-7-(pent-4-ynyloxy)-2H-chromene-3-carboxylate	$(CH_2)_3C{\equiv}CH$	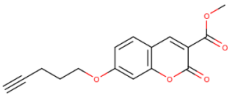	11.56
4a	Methyl 2-oxo-7-(hex-5-ynyloxy)-2H-chromene-3-carboxylate	$(CH_2)_4C{\equiv}CH$	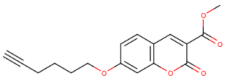	6.83
5a	Methyl 6-(hex-5-ynyloxy)-2-oxo-2H-chromene-3-carboxylate	$(CH_2)_4C{\equiv}CH$	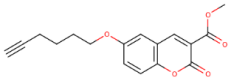	81.30
6a	Methyl 7-(4-chlorophenethoxy)-2-oxo-2H-chromene3-carboxylate	$(CH_2)_2C_6H_4$-4-Cl	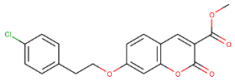	53
7a	Methyl 6-(4-chlorophenethoxy)-2-oxo-2H-chromene3-carboxylate	$(CH_2)_2C_6H_4$-4-Cl	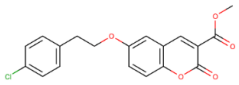	>83.33
8a	Methyl 7-(3-fluorobenzyloxy)-2-oxo-2H-chromene-3carboxylate	$CH_2C_6H_4$-3-F	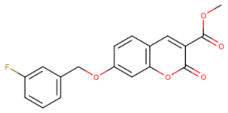	131.29
9a	Methyl 6-(3-fluorobenzyloxy)-2-oxo-2H-chromene-3carboxylate	$CH_2C_6H_4$-3-F	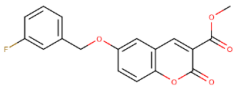	n/a

SI: Selectivity index (IC50 MAO-A/IC50 MAO-B).

Table 2. Chemical structures of R2 derivatives and their MAO inhibitory activities [14]

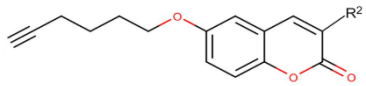
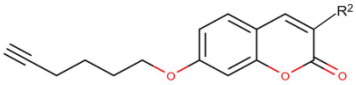

Compound	Nomenclature	R2	Structure	SI
1b	3-(4-Methoxybenzoyl)-7-(hex-5-ynyloxy)-2H-chromen-2-one	COC6H4-4-OMe	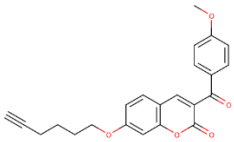	>150
2b	3-(4-Methoxybenzoyl)-6-(hex-5-ynyloxy)-2H-chromen-2-one	COC6H4-4-OMe	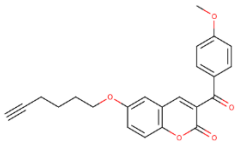	—
3b	N-(2-Oxo-7-(hex-5-ynyloxy)-2H-chromen-3-yl)acetamide	NHCOMe	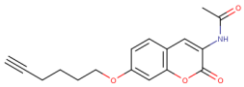	1.6
4b	N-(2-Oxo-6-(hex-5-ynyloxy)-2H-chromen-3-yl)acetamide	NHCOMe	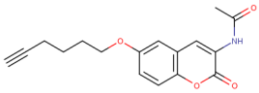	>404.85
5b	7-(Hex-5-ynyloxy)-2H-chromen-2-one	H	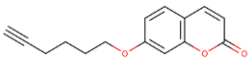	140
6b	7-(Hex-5-ynyloxy)-3-(4-methoxyphenyl)-2H-chromen2-one	C6H4-4-OMe	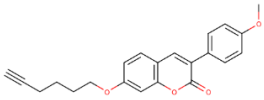	>3378.37

SI: Selectivity index (IC_{50} MAO-A/IC_{50} MAO-B).

The molecules were regrouped into two groups: the first group (1a to 9a) contain R^1 derivatives with a methyl acetate moiety at C3 while the variation occurs at C6 or C7. Meanwhile, the second group (1b to 6b) contain R^2 derivatives with a hex-5-ynyloxy chain at C6 or C7 while the variation occurs at C3 as seen in Figure 2.

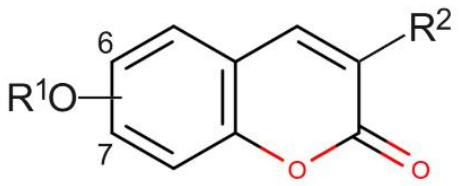

Figure 2. Coumarin scaffold with $R^2 = CO_2Me$ at C3 (1a – 8a) and $R^1 = (CH_2)_4{\equiv}CH$ at C6 or C7 (1b – 6b).

Molecular Docking

Molecular docking was used for analysis of the interactions between the coumarin derivatives, and the active site of MAO-B. Docking simulation was performed by employing the AutoDock Vina 1.1.2 program [17]. The grid box was placed near the FAD with a spacing of 1 Å. Grid dimensions were chosen large enough (24 x 24 x 24 Å in x, y and z directions, respectively) to fit both cavities of the active site in the protein. The grid box was positioned in a way to cover the entire binding site and to allow larger molecules to dock properly (53 x 155 x 27 Å in x, y and z directions, respectively). Conformations of docked ligands were chosen according to their binding affinity and their conformation similarity to the native ligand.

Results

Molecular Docking Results

Conformations of docked compounds were ranked by their energies and then selected based on their similarity to the co-crystallized ligand which is also a coumarin derivative by mean of superposition. Hydrogen bonds were visualized using UCSF Chimera, Discovery Studio Visualizer was used to determine the nearby interacting hydrophobic amino acids [18]. Molecular docking results are shown in Table 3.

Table 3. Molecular docking results of selected ligands with MAO-B

Compound	ΔGb (kcal/mol)	Hydrogen bonds		Hydrophobic interactions
		Residues	Bond length (Å)	
C18	-9.7	Tyr-435	3.0	Trp-119, Leu-164, Leu-167, Phe-168, Leu-171, Ile-199, Tyr-326, Phe-343
1a	-8.9	FAD-1502	2.3	Leu-171, Ile-316, Tyr-326
2a	-9.1	FAD-1502	2.4	Phe-168, Leu-171, Ile-199, Tyr-326, Tyr-398, Tyr-435
3a	-9.1	—	—	Leu-164, Leu-167, Phe-168, Leu-171, Ile-199, Ile-316, Tyr-398, Tyr-435
4a	-9.3	FAD-1502	2.5	Trp-119, Leu-171, Ile-199, Tyr-326, Tyr-398, Tyr-435
5a	-8.1	Cys-172	3.4	Phe-168, Leu-171, Ile-199, Gln-206, Tyr-398, Tyr-435
6a	-10.1	FAD-1502	2.3	Trp-119, Leu-164, Leu-171, Ile-199, Ile-316, Tyr-326
7a	-9.7	—	—	Trp-119, Leu-171, Ile-199, Ile-316, Tyr-326, Tyr-398, Tyr-435
8a	-10.8	FAD-1502	2.4	Leu-171, Ile-199, Ile-316, Tyr-326
9a	-9.7	FAD-1502 Tyr-188	2.6	Ile-199, Ile-316, Pro-102, Pro-104, Gly-434, Leu-171, Cys-172
1b	-8.0	—	—	Phe-103, Trp-119, Leu-164, Leu-167, Leu-171, Ile-199, Ile-316, Tyr-326, Tyr-398, Thr-399, Tyr-435
2b	-6.1	Cys-172	3.4	Trp-119, Leu-164, Phe-168, Leu-171, Ile-199, Ile-316, Tyr-326, Phe-343, Tyr-435
3b	-8.5	—	—	Phe-103, Trp-119, Leu-164, Leu-167, Leu-171, Ile-199, Ile-316, Tyr-398, Tyr-435
4b	-8.9	FAD-1502 Tyr-188	2.2 2.4	Trp-119, Leu-171, Ile-199, Tyr-326, Tyr-398, Tyr-435
5b	-9.2	—	—	Trp-119, Leu-171, Ile-199, Tyr-326
6b	-8.9	—	—	Pro-104, Trp-119, Leu-164, Leu-167, Phe-168, Ile-199, Ile-316, Leu-171, Ile-198, Cys-172, Tyr-326, Gln-206, Tyr-398, Tyr-435, Gly-434, FAD-1502

A good correlation (R^2 = 0.535) was established between docking results and Log of experimental IC_{50} values, which confirms the reliability of the molecular docking approach to study the mode of interaction of coumarin derivatives with MAO-B, the correlation plot and the equation used are shown in Figure 3.

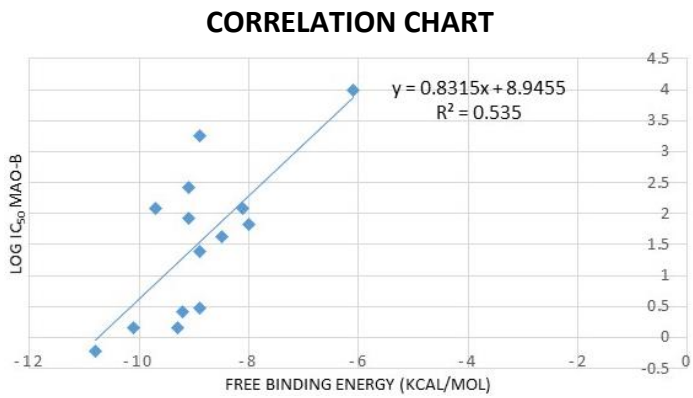

Figure 3. Correlation between docking free binding energy and experimental IC_{50} values.

The docking poses were visualized using UCSF Chimera visualization software and are shown in Figure 4.

An additional docking of safinamide (SAG) was conducted for comparison purpose and the result show that it binds to the Gln-206 as mentioned in the literature with a free binding energy of -10.1 kcal/mol [11]. Whereas the redocking of the co-crystallized coumarin derivative show that it forms a hydrogen bond with Tyr-435 of the aromatic cage. This difference may be due to the absence of water molecules during the docking process.

The fourteen compounds were separated into two groups: R^1 derivatives (1a-9a) with variation occurring in either C6 or C7 and R^2 derivatives (1b-6b) with variation occurring in C3.

The docking poses were visualized using UCSF Chimera visualization software and are shown in Figure 4.

An additional docking of safinamide (SAG) was conducted for comparison purpose and the result show that it binds to the Gln-206 as mentioned in the literature with a free binding energy of -10.1 kcal/mol [11]. Whereas the redocking of the co-crystallized coumarin derivative show that it

forms a hydrogen bond with Tyr-435 of the aromatic cage. This difference may be due to the absence of water molecules during the docking process.

The fourteen compounds were separated into two groups: R^1 derivatives (1a-9a) with variation occurring in either C6 or C7 and R^2 derivatives (1b-6b) with variation occurring in C3.

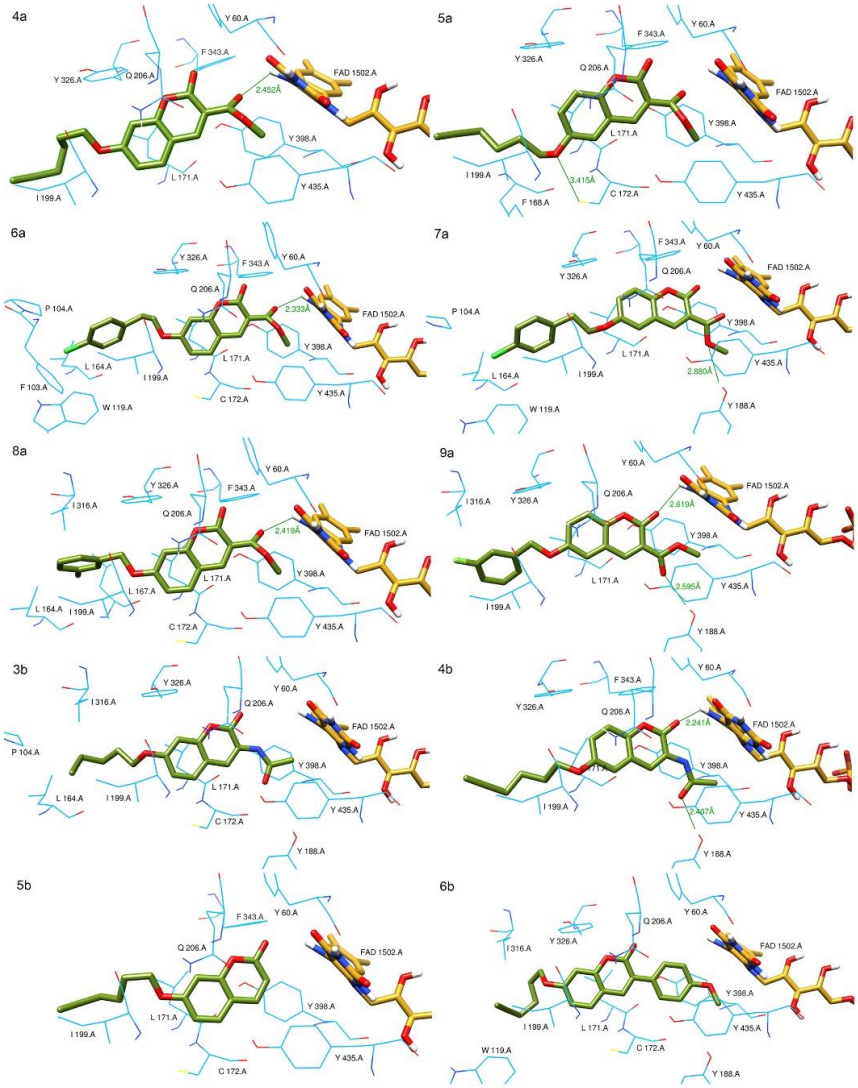

Figure 4. Docking poses of the selected coumarin derivatives within MAO-B active site, hydrogen bonds are shown in green lines.

Structure-Activity Relationship Analysis

To identify the structural requirements for coumarin derivatives to potently and selectively inhibit MAO-B, the first four molecules (1a-4a) were modified by adding a methyl group in the ether chain in each molecule. The ether chain elongation which resulted in an increased molecule length has been shown to be favourable for MAO-B inhibition. Molecular docking showed a significant increase in hydrophobic interactions. MAO-B active site is a long cavity and hence the elongated ether chain allowed the ligand to occupy both cavities and interact with the FAD cofactor through hydrogen bonding as demonstrated in the compound 4a. This compound is considered a dual inhibitor with IC_{50} values of 9.64 nM and 1.41 nM for MAO-A and MAO-B respectively [14].

The compound 5a which is a C7-isomer of 4a has been shown to be slightly less potent with an IC_{50} of 123 nM but more selective towards MAO-B (SI > 81). The structural analysis reveals that the ether chain in the C6-isomer is directed towards the bottom of the entrance cavity and forms a hydrogen bond with the residue Cys-172 which is not present in MAO-A suggesting that this residue may play a role in MAO-B selectivity.

We note that this increase in selectivity due to the replacement of the ether chain in C6 is also noted in the compound 7a. The docking result shows that it binds to the aromatic residue Tyr-188 which is located in the bottom of the aromatic cage through hydrogen bonding. We note that this residue is replaced with a glutamic acid in MAO-A and thus may be involved in MAO-B selectivity.

Lastly, the compound 8a was modified by adding a 4-fluorobenzyloxy moiety in C7, according to the docking result, this ligand is the most stable amongst the selected compounds displaying the lowest binding affinity (-10.8 kcal/mol). We note that this compound was also the most potent with an IC_{50} value of 0.58 nM according to the experimental study [14].

In the compound 9a, a C6-isomer of 8a was modelled and docked for comparison purpose. Our result show that it binds in a similar way to the compound 7a, forming two hydrogen bonds with FAD cofactor and Tyr-188. Detailed SAR analysis is illustrated in Figure 5.

In the second group, the C6-isomer 2b bearing the 1-(4-methoxyphenyl) ethan-1-one at C3 is reported for losing inhibitory activity for both MAO-A and MAO-B, the docking result also shows that this compound binds to MAO-B with the highest binding affinity among the selected compounds. However, the addition of the N-methyl acetamide moiety in the isomers 3b and 4b has

been shown to correlate well with the previous suggestions. The C6-isomer 4b is 400 times more selective for MAO-B compared to its C7-isomer. The binding mode is similar to the previous C6-isomers. Two hydrogen bonds were visualized involving the FAD cofactor and the residue Tyr-188.

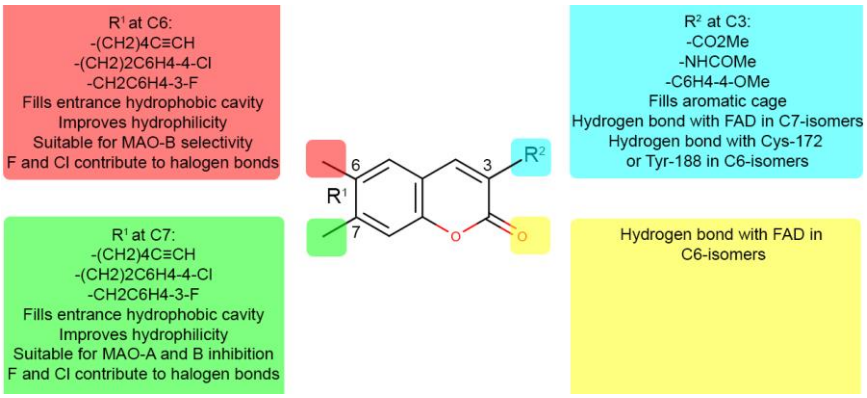

Figure 5. Structure-activity relationship (SAR) analysis of alkynyl coumarinyl ethers.

Finally, the last compounds bearing the hex-5-ynyloxy chain at C7 were compared by adding a 1-methoxy-4-methylbenzene moiety at C3 in the compound 6b while leaving it blank in the compound 5b. The docking result of the compound 6b shows that it binds to MAO-B with a free binding energy of -8.9 kcal/mol. Its experimental IC_{50} value is estimated to 2.96 nM and displays a MAO-B selectivity of over 3400 [14].

The structural analysis shows that the aromatic ring at C3 in the compound 6b occupies the aromatic cage and it's stabilized between the two residues Tyr-398 and Tyr-435. Meanwhile the coumarin ring is involved in π-stacking interactions with the gating residues Ile-199 and Tyr-326. Other hydrophobic interactions are shown in Table 3.

Discussion

Based on previously reported experimental data, it was confirmed that C7-isomers of coumarins tend to be more potent towards MAO-B, meanwhile the C6-isomers are slightly less potent but tend to be more selective towards MAO-B isoform [14]. We noticed that this hypothesis is applied to the

compounds: 4a, 6a and 3b and their respective C6-isomers: 5a, 7a and 4b which displayed a MAO-B selectivity of approximately 80, 80 and 400-fold respectively. Due to the absence of compound 8a isomer, we used molecular modeling to design a C6-isomer of this compound and was docked within MAO-B active site. Structural analysis revealed that it binds in a similar way to other C6-isomers, with the 4-fluorobenzyloxy moiety directed towards the bottom of the cavity and engaging the residue Tyr-188 in a hydrogen bond with the oxygen of the methyl acetate moiety at C3, meanwhile the oxygen of coumarin scaffold established a hydrogen bond with the cofactor FAD as observed in most compounds. However, an *in vitro* inhibition assay is required to determine its MAO-B selectivity.

Structural analysis of the most selective compound, 6b, revealed that it does not bind to MAO-B active site through any hydrogen bonds but establishes hydrophobic interactions involving various residues of the hydrophobic pocket which seems to be more favorable for the stability of the protein-ligand complex than any other interactions such as hydrogen or halogen bonds. Furthermore, the long shape of the molecule plays a role in its selectivity as the differences between MAO-A and MAO-B are mainly related to the shape and the flexibility of their active site cavities. The long and narrow cavity of MAO-B makes it preferentially bind long inhibitors which forces a conformational change of the gating residue Ile-199 and fuses the two cavities into one [19-21]. The absence of this mechanism in MAO-A isoform further strengthen this hypothesis and could explain why such inhibitors tend to be more selective towards MAO-B.

Moreover, the molecular docking study further confirmed that all coumarin derivatives bind non-covalently to MAO-B active site and the triple bond of the ether chain doesn’t bind to the cofactor FAD as such in irreversible inhibitors.

Conclusion

The current study aimed to shed a light on the mode of interaction of previously reported alkynyl coumarinyl ethers at the molecular level. It was found that C6-isomers are more selective towards MAO-B compared to their respective C7-isomers. Structure-activity relationship revealed that the loss of activity towards MAO-A of these compounds may be due to the bulky side chain of Phe-208 which is replaced by the gating residue Ile-199 that displays

a conformational change depending on the nature of the inhibitor. Among the studied ligands, the compound 6b is considered the best drug-candidate among the fourteen compounds which needs more focus for the development of new antiparkinsonian drugs in respect to its drug likeness, high potency and selectivity for MAO-B.

Disclaimer

None.

References

[1] Noda, S., Sato, S., Fukuda, T., Tada, N., Uchiyama, Y., Tanaka, K., & Hattori, N. (2020). Loss of Parkin contributes to mitochondrial turnover and dopaminergic neuronal loss in aged mice. *Neurobiology of Disease*, 136, 104717

[2] Poewe, W., & Mahlknecht, P. (2020). Pharmacologic Treatment of Motor Symptoms Associated with Parkinson Disease. *Neurologic Clinics*, 38(2), 255-267.

[3] Dorsey, E. R., Elbaz, A., Nichols, E., Abd-Allah, F., Abdelalim, A. Adsuar, J. C., Mustafa Geleto Ansha, Carol Brayne, Jee-Young J Choi, Daniel Collado-Mateo, Nabila Dahodwala, Huyen Phuc Do, Dumessa Edessa, Matthias Endres, Seyed-Mohammad Fereshtehnejad, Kyle J Foreman, Fortune Gbetoho Gankpe, Rahul Gupta, Samer Hamidi, Graeme J. Hankey, Simon I. Hay, Mohamed I Hegazy, Desalegn T. Hibstu, Amir Kasaeian, Yousef Khader, Ibrahim Khalil, Young-Ho Khang, Yun Jin Kim, Yoshihiro Kokubo, Giancarlo Logroscino, João Massano, Norlinah Mohamed Ibrahim, Mohammed A. Mohammed, Alireza Mohammadi, Maziar Moradi-Lakeh, Mohsen Naghavi, Binh Thanh Nguyen, Yirga Legesse Nirayo, Felix Akpojene Ogbo, Mayowa Ojo Owolabi, David M. Pereira, Maarten J Postma, Mostafa Qorbani, Muhammad Aziz Rahman, Kedir T. Roba, Hosein Safari, Saeid Safiri, Maheswar Satpathy, Monika Sawhney, Azadeh Shafieesabet, Mekonnen Sisay Shiferaw, Mari Smith, Cassandra E I Szoeke, Rafael Tabarés-Seisdedos, Nu Thi Truong, Kingsley Nnanna Ukwaja, Narayanaswamy Venketasubramanian, Santos Villafaina, Kidu Gidey Weldegwergs, Ronny Westerman, Tissa Wijeratne, Andrea S. Winkler, Bach Tran Xuan, Naohiro Yonemoto, Valery L Feigin, Theo Vos, Christopher J L Murray. (2018). Global, reginal, and national burden of Parkinson's disease, 199-2016: a systematic analysis for the Global Burden of Disease Study 2016. *The Lancet Neurology*, 17(11), 939-953.

[4] Youdim, M. B., Edmondson, D., & Tipton, K. F. (2006). The therapeutic potential of monoamine oxidase inhibitors. *Nature reviews neuroscience*, 7(4), 295-309.

[5] Shih, J. C., Chen, K., & Ridd, M. J. (1999). Monoamine oxidase: from genes to behavior. *Annual review of neuroscience*, 22(1), 197-217.

[6] Youdim, M. B., Edmondson, D., & Tipton, K. F. (2006). The therapeutic potential of monoamine oxidase inhibitors. *Nature reviews neuroscience*, 7(4), 295-309.

[7] Culpepper, L. (2013). Reducing the burden of difficult-to-treat major depressive disorder: revisiting monoamine oxidase inhibitor therapy. *The primary care companion for CNS disorders*, 15(5).

[8] Youdim, M. B., Gross, A., & Finberg, J. P. (2001). Rasagiline [N-propargyl-1R (+)-aminoindan], a selective and potent inhibitor of mitochondrial monoamine oxidase B. *British journal of pharmacology*, 132(2), 500-506.

[9] Jenner, P., & Olanow, C. W. (1996). Oxidative stress and the pathogenesis of Parkinson's disease. *Neurology*, 47(6 Suppl 3), 161S-170S.

[10] Son, S. Y., Ma, J., Kondou, Y., Yoshimura, M., Yamashita, E., & Tsukihara, T. (2008). Structure of human monoamine oxidase A at 2.2-Å resolution: the control of opening the entry for substrates/inhibitors. *Proceedings of the National Academy of Sciences*, 105(15), 5739-5744.

[11] Binda, C., Wang, J., Pisani, L., Caccia, C., Carotti, A., Salvati, P., Dale E. Edmondson, & Mattevi, A. (2007). Structures of human monoamine oxidase B complexes with selective noncovalent inhibitors: safinamide and coumarin analogs. *Journal of medicinal chemistry*, 50(23), 5848-5852.

[12] Stefanachi, A., Leonetti, F., Pisani, L., Catto, M., & Carotti, A. (2018). Coumarin: A natural, privileged and versatile scaffold for bioactive compounds. *Molecules*, 23(2), 250.

[13] Gnerre, C., Catto, M., Leonetti, F., Weber, P., Carrupt, P. A., Altomare, C., A Carotti & Testa, B. (2000). Inhibition of monoamine oxidases by functionalized coumarin derivatives: biological activities, QSARs, and 3D-QSARs. *Journal of medicinal chemistry*, 43(25), 4747-4758.

[14] Mertens, M. D., Hinz, S., Müller, C. E., & Gütschow, M. (2014). Alkynyl-coumarinyl ethers as MAO-B inhibitors. *Bioorganic & medicinal chemistry*, 22(6), 1916-1928.

[15] Edmondson, D. E., Binda, C., & Mattevi, A. (2004). The FAD binding sites of human monoamine oxidases A and B. *Neurotoxicology*, 25(1-2), 63-72.

[16] Pettersen, E. F., Goddard, T. D., Huang, C. C., Couch, G. S., Greenblatt, D. M., Meng, E. C., & Ferrin, T. E. (2004). UCSF Chimera - a visualization system for exploratory research and analysis. *Journal of computational chemistry*, 25(13), 1605-1612.

[17] Trott, O., & Olson, A. J. (2010). AutoDock Vina: improving the speed and accuracy of docking with a new scoring function, efficient optimization, and multithreading. *Journal of computational chemistry*, 31(2), 455-461.

[18] Systèmes, D. (2016). *Biovia, discovery studio modeling environment*. Dassault Systèmes Biovia: San Diego, CA, USA.

[19] Finberg, J. P., & Rabey, J. M. (2016). Inhibitors of MAO-A and MAO-B in psychiatry and neurology. *Frontiers in pharmacology*, 7, 340.

[20] Boulaamane, Y., Ahmad, I., Patel, H., Das, N., Britel, M. R., & Maurady, A. (2022). Structural exploration of selected C6 and C7-substituted coumarin isomers as

selective MAO-B inhibitors. *Journal of Biomolecular Structure and Dynamics*, 1-15.

[21] Boulaamane, Y., Ibrahim, M. A., Britel, M. R., & Maurady, A. (2022). *In silico* studies of natural product-like caffeine derivatives as potential MAO-B inhibitors/AA2AR antagonists for the treatment of Parkinson's disease. *Journal of Integrative Bioinformatics*.